

Tibetan singing bowls

This article has been downloaded from IOPscience. Please scroll down to see the full text article.

2011 Nonlinearity 24 R51

(<http://iopscience.iop.org/0951-7715/24/8/R01>)

View [the table of contents for this issue](#), or go to the [journal homepage](#) for more

Download details:

IP Address: 194.254.61.1

The article was downloaded on 01/07/2011 at 16:44

Please note that [terms and conditions apply](#).

INVITED ARTICLE

Tibetan singing bowls

Denis Terwagne¹ and John W M Bush²¹ GRASP, Département de Physique, Université de Liège, B-4000 Liège, Belgium² Department of Mathematics, Massachusetts Institute of Technology, 02139 Cambridge, MA, USA

Received 8 April 2010

Published 1 July 2011


Online at stacks.iop.org/Non/24/R51

Recommended by D Lohse

Abstract

We present the results of an experimental investigation of the acoustics and fluid dynamics of Tibetan singing bowls. Their acoustic behaviour is rationalized in terms of the related dynamics of standing bells and wine glasses. Striking or rubbing a fluid-filled bowl excites wall vibrations, and concomitant waves at the fluid surface. Acoustic excitation of the bowl's natural vibrational modes allows for a controlled study in which the evolution of the surface waves with increasing forcing amplitude is detailed. Particular attention is given to rationalizing the observed criteria for the onset of edge-induced Faraday waves and droplet generation via surface fracture. Our study indicates that drops may be levitated on the fluid surface, induced to bounce on or skip across the vibrating fluid surface.

Mathematics Subject Classification: 74-05, 76-05

 Online supplementary data available from stacks.iop.org/Non/24/R51/mmedia

(Some figures in this article are in colour only in the electronic version)

1. Introduction

Tibetan singing bowls are thought to have originated from Himalayan fire cults of the 5th century BC and have since been used in various religious ceremonies, including shamanic journeying and meditation. The Tibetan singing bowl (see figure 1 and the supplementary data (movie 1) available at stacks.iop.org/Non/24/R51/mmedia) is a type of standing bell played by striking or rubbing its rim with a wooden or leather-wrapped mallet. This excitation causes the sides and rim of the bowl to vibrate and produces a rich sound. Tibetan bowls are hand made and their precise composition is unknown, but generally they are made of a bronze alloy that can include copper, tin, zinc, iron, silver, gold and nickel. When the bowl is filled with water, excitation can cause ripples on the water surface. More vigorous forcing generates progressively more complex surface wave patterns and ultimately the creation of droplets via



Figure 1. Our Tibetan singing bowls: (a) Tibet 1, (b) Tibet 2, (c) Tibet 3 and (d) Tibet 4.

wave breaking. We here quantify this evolution, and demonstrate the means by which the Tibetan singing bowl can levitate droplets.

Related phenomena are known to appear in other vessels, including the Chinese singing bowl, on which vibrations are generated by rubbing the vessel's handles with moistened hands. The more familiar vibration of a wine glass is produced by rubbing its rim with a moist finger. The dependence of the glass's vibration frequency on its material properties, geometry and characteristics of the contained fluid was elucidated by French [1] and subsequent investigators [2–5]. The coupling between two singing wine glasses has been investigated by Arane *et al* [6]. Apfel [7] demonstrated experimentally that wine glass vibration generates capillary waves near the walls of a fluid-filled glass. Moreover, he made the connection between these waves and the acoustic whispering gallery modes elucidated by Rayleigh [8]. By studying the deformation and the sound spectrum produced by a single wine glass, Rossing [9] elucidated the mechanism of the glass harmonica [10], an instrument designed by Benjamin Franklin. Joubert *et al* [11] provided a theoretical rationale for observations of standing waves in a singing wine glass. The Tibetan singing bowl has to date received relatively little attention. Inacio *et al* examined experimentally the acoustic response of bowls excited by impact and rubbing [12], and proposed a dynamical formulation of the bowl and presented some numerical simulations [13]. The hydrodynamics of a fluid-filled Tibetan bowl will be the focus of our investigation.

In 1831, Faraday [14] demonstrated that when a horizontal fluid layer is vibrated vertically, its interface remains flat until a critical acceleration is exceeded. Above this threshold, a field of waves appears at the interface, parametric standing waves oscillating with half the forcing frequency [15–20]. The form of such Faraday waves depends on the container geometry; however, boundary effects can be minimized by using a large container. The Faraday waves have a wavelength prescribed by the relative importance of surface tension and gravity, being capillary and gravity waves in the short and long wavelength limits, respectively. As the forcing acceleration is increased, progressively more complex wave patterns arise, and the interfacial dynamics become chaotic [19–21]. Ultimately, large amplitude forcing leads to surface fracture and the ejection of droplets from the fluid bath. A recent study on the breaking of Faraday waves in a vertically shaken bath has been performed in both the capillary and gravity wave limits by Puthenveetil and Hopfinger [22]. Goodridge *et al* [23] studied the drop ejection threshold of capillary waves in a glycerine–water solution for frequencies up to 100 Hz.

Faraday [14] reported that such parametric waves can also be emitted by a vertical plate plunged into a liquid bath and shaken horizontally: along both sides of the plate, waves aligned perpendicular to the plate oscillate at half the forcing frequency. These so-called cross waves, or edge-induced Faraday waves, are typically produced by a wave

maker, and have received considerable attention [24–28]. Hsieh [29] examined theoretically wave generation in a vibrating circular elastic vessel, specifically the axisymmetric capillary waves and circumferential ripples that appear in an inviscid fluid subject to radial wall displacement. These studies have demonstrated that the excitation of the cross waves is due to a parametric resonance. The complexity of this problem lies in the nonlinear interactions between the motion of the oscillating rim and the resulting wave field.

Droplets ejected on the liquid surface by breaking Faraday waves may bounce, skid and roll before coalescing. A number of recent studies have examined droplets bouncing on a vertically vibrating liquid bath below the Faraday threshold [30–32]. The air film between the drop and the liquid surface is squeezed and regenerated at each successive bounce, its sustenance precluding coalescence and enabling droplet levitation. A similar effect arises on a soap film, a system more readily characterized theoretically [35]. The bouncing periodicity depends on the size of the drop and the vertical forcing acceleration of the bath [33, 34]. Couder *et al* [30] have shown that, through the waves emitted at previous bounces, some droplets can walk horizontally across the liquid surface. Several factors are needed to sustain a so-called ‘walker’ [36]. First, the drop must bounce at half the forcing frequency, so that it resonates with the resulting Faraday wave field. Second, the bath must be close to the Faraday instability threshold so that Faraday waves of large amplitude and spatial extent can be excited by the drop impacts. The droplet bounces on the slope of the wave emitted at the previous bounce and so receives an impulsive force in a specific direction, along which it walks with a constant speed. Such walkers have both wave and particle components, and have been shown to exhibit quantum-like dynamical behaviour previously thought to be peculiar to the microscopic realm [37–40]. Might such modern physics arise in our ancient bowls?

The paper is divided into two main parts. In section 2, we examine the acoustics of the Tibetan singing bowls. We begin in section 2.1 by reviewing the related dynamics and theoretical description of the wine glass [1]. In section 2.2, our bowls are presented and their deformation spectra analysed. Then, by adapting the theoretical description of the vibrating wine glass, we infer the Young’s modulus of the alloy comprising our bowls. In section 3, we examine the dynamics of flows generated within liquid-filled vibrating bowls. A review of Faraday waves and droplet ejection on a vertically shaken bath is presented in section 3.1. In section 3.2, our experimental technique is detailed. In section 3.3, we analyse the surface waves generated on the liquid bath, and their relation to Faraday waves. In section 3.4, we examine the limit of large amplitude forcing, in which droplets are ejected by breaking Faraday waves. Comparisons are made with experiments performed on a vertically shaken liquid bath. Droplet levitation is considered in section 3.5, where particular attention is given to developing criteria for droplet bouncing and exploring the possibility of walking droplets. A summary of our results is presented in section 4.

2. Acoustics

2.1. Background

Both the wine glass and the Tibetan bowl can be excited by either tapping or rubbing its rim. We denote by (n, m) the vibrational mode with n complete nodal meridians and m nodal parallels. Tapping excites a number of vibrational modes [10], while rubbing excites primarily the (2,0) fundamental mode (see figure 2(b)). Entirely flexural motion implies radial and tangential displacements proportional to $n \sin n\theta$ and $\cos n\theta$, respectively, θ being the azimuthal coordinate [41]. For the (2,0) mode the maximum tangential motion is necessarily half the maximum normal motion.

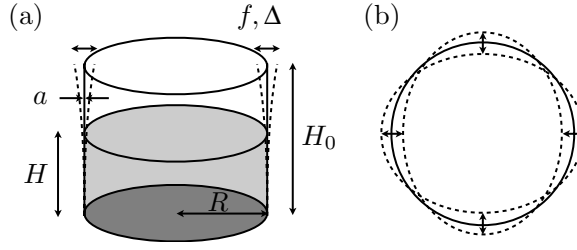


Figure 2. (a) Schematic illustration of a vibrating vessel filled with liquid. Relevant parameters are the height H_0 and the radius R of the vessel, the thickness of the rim a , the liquid level H , the frequency f and the amplitude Δ of the oscillating rim. (b) Top view of a vibrating vessel in its fundamental mode (2,0), characterized by its 4 nodes and 4 antinodes.

A leather mallet can excite bowl vibrations via a stick-slip process, as does a finger moving on a wine glass. The moving mallet forces the rim to follow the mallet during the stick phase; during the slip phase, the bowl rim relaxes to its equilibrium position. This rubbing results in a sound composed of a fundamental frequency plus a number of harmonics. While the mallet is in contact with the bowl, one of the nodes follows the point of contact [11], imparting angular momentum to the bound liquid.

To simplify the acoustic analysis, one can approximate the glass or bowl by a cylindrical shell with a rigid base and an open top (figure 2(a)). The system can then be described in terms of 7 physical variables, the radius R , height H_0 , thickness a , Young's modulus Y and density ρ_s of the cylindrical shell, and the frequency f and amplitude Δ of its oscillating rim. The system can thus be described in terms of 4 independent dimensionless groups, which we take to be R/H , Δ/a , Δ/R and a Cauchy number $Ca = \rho_s f^2 \Delta^2 / Y$ that indicates the relative magnitudes of the inertial and the elastic forces experienced by the vibrating rim.

The sound is emitted by bending waves that deform the rim transversely as they propagate. The speed V_b of bending waves on a two-dimensional plate of thickness a is given by [42]

$$V_b = \left(\frac{\pi V_L f a}{\sqrt{3}} \right)^{1/2}, \quad (1)$$

where V_L is the longitudinal wave speed in the solid (approximately 5200 m s^{-1} in glass). In order for the bending wave to traverse the perimeter in an integer multiple of the period, we require

$$\frac{1}{f} \propto \frac{2\pi R}{V_b}. \quad (2)$$

Thus, since $V_b \sim \sqrt{f a}$, we have $f \propto a/R^2$: the frequency increases with rim thickness, but decreases with radius.

A more complete theoretical analysis of the wine glass acoustics [1] can be applied to our Tibetan bowls. An ideal cylinder fixed at the bottom is considered (figure 2(a)), its wall vibrating with largest amplitude at its free edge or rim. The rim's kinetic energy and elastic energy of bending in the mode (2,0) are calculated by assuming that the radial position is proportional to $\cos 2\theta$, with θ being the azimuthal coordinate. By considering conservation of total energy (kinetic plus elastic bending energy), an expression for the frequency of this mode can be deduced:

$$f_0 = \frac{1}{2\pi} \left(\frac{3Y}{5\rho_s} \right)^{1/2} \frac{a}{R^2} \left[1 + \frac{4}{3} \left(\frac{R}{H_0} \right)^4 \right]^{1/2}. \quad (3)$$

Table 1. Physical properties of the four Tibetan bowls used in our study.

Bowl name	Tibet 1	Tibet 2	Tibet 3	Tibet 4
Symbol	●	○	⊠	◇
$f_{(2,0)}$ (empty) (Hz)	236	187	347	428
Radius R (cm)	7.5	8.9	6	5.9
Thickness a (cm)	0.34	0.38	0.31	0.37
Mass (kg)	0.690	0.814	0.306	0.312
Volume (cm ³)	76	97	35	33
Density (kg m ⁻³)	9079	8366	8754	9372

When the bowl is partially filled with liquid to a depth H (figure 2(a)), the frequency decreases. French [1] captured this effect by considering the kinetic energy of the liquid near the rim, and so deduced the frequency of the fundamental mode:

$$\left(\frac{f_0}{f_H}\right)^2 \sim 1 + \frac{\alpha}{5} \frac{\rho_l R}{\rho_s a} \left(\frac{H}{H_0}\right)^4, \quad (4)$$

where ρ_l is the liquid density and $\alpha \sim 1.25$ is a constant indicating the coupling efficiency between the rim and fluid displacements. Similarly, frequencies of higher modes can be calculated by considering a radial position proportional to $\cos n\theta$ and with m nodal parallels [1]:

$$f_{(n,m)} = \frac{1}{12\pi} \left(\frac{3Y}{\rho_s}\right)^{1/2} \frac{a}{R^2} \left[\frac{(n^2 - 1)^2 + (mR/H_0)^4}{1 + 1/n^2} \right]^{1/2}. \quad (5)$$

2.2. Tibetan bowls

Four different antique bowls of different sizes have been studied (figure 1). They are referred to as Tibet 1, 2, 3 and 4 and their physical characteristics are reported in table 1.

When a bowl is struck or rubbed, the sound emitted by the resulting bowl vibrations is recorded with a microphone and a fast Fourier transform performed on the signal. Different peaks clearly appear in the frequency spectrum, corresponding to the bowl's different vibrational modes. Figure 3(a) indicates the frequency spectrum generated by striking the empty bowl Tibet 4. When the bowl is rubbed with a leather-wrapped mallet, the lowest mode is excited along with its harmonics, an effect known as a mode 'lock in' [43]. The frequency spectrum of Tibet 4 when rubbed by a leather mallet is presented in figure 3(b). Due to the bowl asymmetry, two peaks separated by several Hz arise and a beating mode is heard. This split is highlighted in a magnification of the first peak $f_{(2,0)}$ in the inset of the figure. The deformation shapes are the same with both frequencies but there is horizontal angular shift observed to be $\pi/4$ between them for the fundamental modes $(2, 0)$ and $\pi/2n$ for other $(n, 0)$ modes. Finally, we note that, owing to the relative squatness of the bowls and the associated high energetic penalty of modes with $m \neq 0$, only modes $(n, 0)$ were excited; henceforth, such modes are denoted simply by n .

We can also find a relation between the different mode frequencies. Since the speed of the bending wave is proportional to the square root of the frequency, $v \propto \sqrt{f}$ and since $\lambda = v/f$, we expect $\lambda \propto 1/\sqrt{fa}$. For the mode n , we thus have $2\pi R = n\lambda_n$. The frequency of this mode n should thus be proportional to

$$f \propto \frac{n^2 a}{R^2}. \quad (6)$$

In figure 4(a), resonant frequencies of the 4 bowls are plotted as a function of their corresponding mode n and a power 2 curve is fit onto each curve. In figure 4(b), we collapse

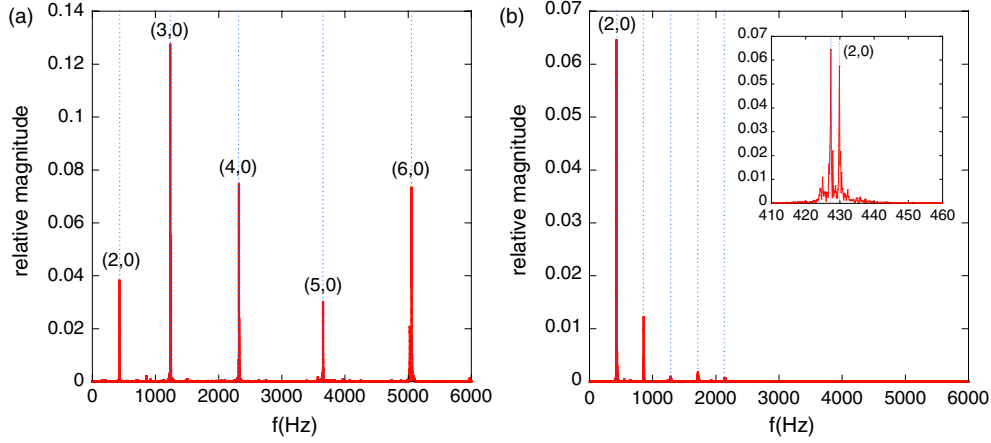


Figure 3. (a) Frequencies excited in the bowl Tibet 4 when struck with a wooden mallet. The different peaks correspond to the natural resonant frequencies of the bowl, and the associated deformation modes (n, m) are indicated. (b) Excited frequencies of the bowl Tibet 4 when rubbed with a leather mallet. The first peak corresponds to the deformation mode $(2,0)$ and subsequent peaks to the harmonics induced by mode lock-in. In the inset, a magnification of the first peak provides evidence of its splitting due to the asymmetry of the bowl.

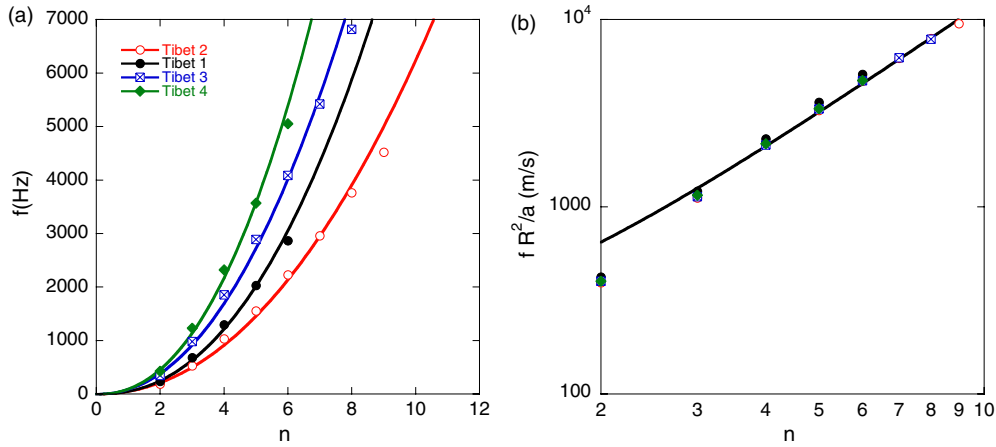


Figure 4. (a) Measurements of the resonant frequencies of the different deformation modes n for the 4 different Tibetan bowls. (b) Characteristic speed fR^2/a as a function of deformation mode n for the 4 different bowls. Data are fit by a power 2 curve indicating that $f_n \propto n^2 a/R^2$, consistent with equation (6).

all these curves onto a line by plotting the characteristic speed fR^2/a as a function of the mode n , thus validating the proposed scaling (6).

It is readily observed that the resonant frequencies decrease when liquid is poured into a vessel. In the inset in figure 5(a), we report the measurements of the fundamental frequency of the bowl Tibet 1 as a function of the dimensionless liquid height H/H_0 . In figure 5(a), we report $(f_0/f_H)^2$ as a function of $(H/H_0)^4$. According to (4), the slope of this curve gives the ratio $\frac{\alpha}{5} \frac{\rho_l R}{\rho_s a}$. In figure 5(b), we present the dependence of $(1 + 1/n^2)(R^2/a)^2 f^2$ on $(n^2 - 1)^2$ for the deformation modes $n = 2$ through 6 of the bowls Tibet 1, 2, 3 and 4. According to (5),

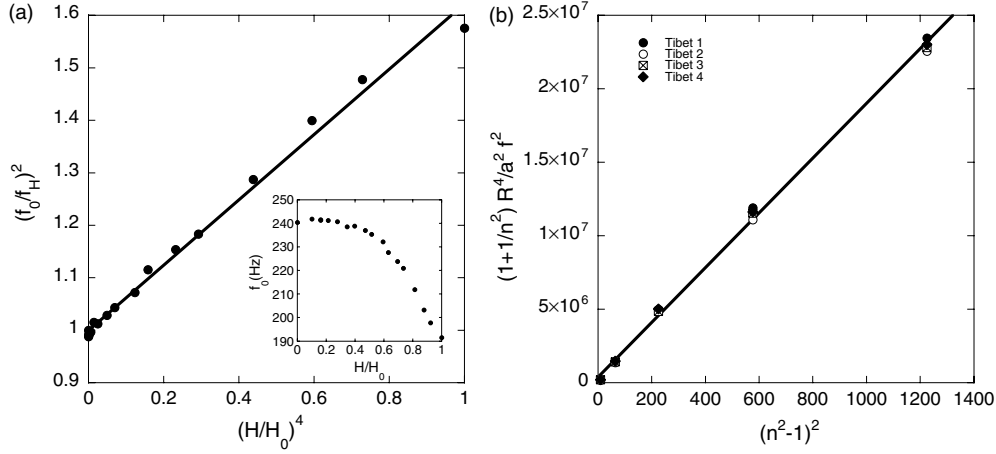


Figure 5. (a) The fundamental frequency of Tibet 1's mode (2,0) as a function of the water height H/H_0 . According to equation (4), the slope is equal to $\frac{\alpha \rho_l R}{5 \rho_s a}$. (b) The dependence of the resonant frequencies f of all the bowls on the deformation mode n may be used to infer the ratio Y/ρ_s . According to (5), the slope of the line shown is $\frac{1}{48\pi^2} \frac{Y}{\rho_s}$, from which we infer $Y/\rho_s = 8.65 \times 10^6 \text{ Pa m}^3 \text{ kg}^{-1}$.

the slope should be equal to $\frac{1}{48\pi^2} \frac{Y}{\rho_s}$. For each value of the abscissa there are 4 measurements corresponding to the 4 Tibetan bowls. Data points from the different Tibetan bowls overlie each other, especially at low n , indicating that all bowls have the same value of ratio Y/ρ_s , and so are likely made of the same material. A linear fit gives $Y/\rho_s = 8.65 \times 10^6 \text{ Pa m}^3 \text{ kg}^{-1}$.

We can simply estimate the density for each Tibetan bowl by measuring its mass and volume. Masses are measured by a weight scale with an error of 2 g while bowl volumes are deduced by fluid displacement during submersion. The error made on the volume with this method is estimated to be no more than 5%. All such density measurements are reported in table 1. Taking the mean value of the densities, equal to 8893 kg m^{-3} , we calculate a Young modulus $Y = 77 \pm 6\% \text{ GPa}$. This value is in the Young's modulus range of glasses and lower than typical brass, copper or bronze alloys for which $Y > 100 \text{ GPa}$.

3. Fluid dynamics

3.1. Faraday waves

Consider an inviscid fluid of density ρ and surface tension σ in a horizontal layer of uniform depth h in the presence of a gravitational acceleration g . The layer is oscillated vertically in a sinusoidal fashion at a forcing frequency $f_0 = \omega_0/2\pi$, amplitude Δ and acceleration $\Gamma g = \Delta\omega^2$. Above a critical forcing acceleration, standing Faraday waves appear on the surface. The associated surface deformation $a(x, y, t)$ can be expressed in terms of the container's eigenmodes $S_m(x, y)$ as

$$a(x, y, t) = \sum_m a_m(t) S_m(x, y), \quad (7)$$

with $a_m(t)$ being the oscillating amplitude of the eigenmode m . Benjamin and Ursell [16] demonstrate that the coefficients $a_m(t)$ satisfy

$$\ddot{a}_m + \omega_m^2 (1 - 2\gamma \cos \omega_0 t) a_m = 0, \quad (8)$$

where

$$\omega_m^2 = \left(gk_m + \frac{\sigma}{\rho} k_m^3 \right) \tanh(k_m h) \quad (9)$$

represents the classic gravity-capillary wave dispersion relation,

$$\gamma = \frac{\Gamma}{2(1 + Bo^{-1})} \quad (10)$$

is the dimensionless forcing acceleration, and $Bo = \frac{\rho g}{\sigma k^2}$ is the Bond number. $k_m = 2\pi/\lambda_m$ is the wave number of the mode m , and λ_m is the corresponding wavelength.

In the absence of forcing, $\Gamma = 0$, (8) describes a simple harmonic oscillation with frequency prescribed by (9) corresponding to the free surface vibrations of the liquid. When $\Gamma > 0$, (8) describes a parametric oscillator as the forcing term depends on time. The resulting Faraday waves can be either capillary or gravity waves according to the magnitude of Bo ; specifically, the former and latter arise in the respective limits $Bo \ll 1$ and $Bo \gg 1$. Equation (8) is known as the Mathieu equation and cannot be solved analytically since one of the terms is time dependent. However, as the forcing is periodic, Floquet theory can be applied to show that an inviscid fluid layer is always unstable to Faraday waves with a frequency ω_F that is half the forcing frequency $\omega_0 = 2\omega_F$ [16]. In the deep water ($kh \gg 1$), capillary wave ($Bo \ll 1$) limit, we can infer from (9) a Faraday wavelength:

$$\lambda_F = (2\pi)^{1/3} (\sigma/\rho)^{1/3} (f_0/2)^{-2/3}. \quad (11)$$

To incorporate the influence of the fluid viscosity, one can add to (8) a phenomenological dissipation term proportional to the velocity [18]:

$$\ddot{a}_m + 2\beta\dot{a}_m + \omega_m^2(1 - 2\gamma \cos \omega_0 t)a_m = 0, \quad (12)$$

where β is the dissipation rate. This dissipation term leads to an acceleration threshold for the Faraday instability. Assuming capillary waves in an unbounded and infinite depth liquid, the critical acceleration needed to induce parametric instability is given by

$$\Gamma_F \propto \frac{1}{g} (\rho/\sigma)^{1/3} \nu \omega_0^{5/3}, \quad (13)$$

where ν is the kinematic viscosity of the fluid [19, 44].

As the forcing amplitude is further increased, the Faraday wave amplitude increases progressively until the waves become chaotic. Ultimately, the waves break and droplets are ejected from the surface. Since drops will be ejected by the breaking of Faraday waves, we expect their diameter to scale as

$$d_m \sim \lambda_F \sim (\sigma/\rho)^{1/3} f_0^{-2/3} \quad (14)$$

in the capillary wave limit. Droplet ejection arises when the destabilizing inertial driving force $m\Gamma g$ (with $m \sim \rho\lambda_F^3$) exceeds the stabilizing surface tension force $\pi\lambda_F\sigma$. This implies, via (14), a threshold acceleration that scales as

$$\Gamma_d \sim 1/g(\sigma/\rho)^{1/3} f_0^{4/3}. \quad (15)$$

The range of validity of these scalings will be investigated in our experimental study.

3.2. Experimental technique

The experimental setup used for studying the surface waves generated within the Tibetan bowls is presented in figure 6. A loudspeaker is set in front of the bowl, its signal received from



Figure 6. Experimental setup. The bowl deformation is excited by a loudspeaker emitting sound at a frequency corresponding to a particular vibrational mode of the bowl. The deformation of the bowl is measured by an accelerometer glued to the bowl's outer wall at the height of the liquid surface.

a signal function generator then amplified. When the applied signal frequency is close to one of the bowl's resonant frequencies, it oscillates in the corresponding deformation mode. Conveniently, with this method, we can select a single deformation mode. Recall that by striking or rubbing the bowls, we excited several modes (figure 3): moreover, rubbing induced a rotational motion that followed the mallet. We can now examine the vibration-induced flows in a controlled fashion.

In order to extend the range of natural frequencies, we consider Tibetan bowls, wine glasses and soda cans (with their tops removed), whose resonant frequencies span a broad range from 50 to 750 Hz. For each, we can vary the resonant frequency by filling it with liquid. The sound emitted by the loudspeaker was not powerful enough to induce significant oscillations of the soda can rim, a problem we eliminated by directly connecting the vibrating membrane of the loudspeaker to the rim of the soda can with a rigid rod.

We measure the acceleration of the rim at an antinode by gluing a lightweight accelerometer (PCB-Piezotronics, 352C65) on the bowl's rim at the level of the liquid surface. In the following, we characterize the sinusoidal rim oscillation by the dimensionless acceleration Γ defined as the maximal acceleration of the rim normalized by the gravitational acceleration $\Gamma = \Delta\omega^2/g$. For wine glasses, the accelerometer cannot be used since it dramatically alters the resonant frequency. We thus used a light weight strain gauge, whose effect on the resonance frequency is negligible.

The strain gauge system provides a measurement of the local extension length of the rim at an antinode. The length variation of the strain gauge is deduced by measuring its electrical resistance with a Wheatstone bridge. To deduce the acceleration of the radial rim movement, we deduce a relation between the longitudinal extension ϵ and the radial amplitude of the rim Δ . Then, the acceleration Γ can be readily deduced. The validity of this indirect method was tested on Tibet 1. An accelerometer was glued next to a strain gauge at an antinode of the bowl Tibet 1. From the strain gauge measurement, we deduced an acceleration that we compared with the direct measurement from the accelerometer. These two independent measurements match well for a wide range of accelerations.

French [1] gives a relation for the convex change of length δl of a curved segment of thickness a as a function of the initial mean radius of curvature R and the deformed radius of curvature r_c : $\delta l = l_0 \frac{a}{2} (\frac{1}{r_c} - \frac{1}{R})$ where l_0 is the initial segment length. Since the deformation is small, we can approximate: $\frac{1}{r_c} \sim \frac{1}{R} + \frac{3x}{R^2}$ where x is the radial displacement of the wall [1]. The strain gauge gives the measurement of the convex longitudinal extension of the rim $\epsilon = \delta l/l_0$. We can thus deduce the maximal radial amplitude of the rim deformation [1]: $x_m = \frac{2}{3} \frac{R^2}{a} \epsilon$.

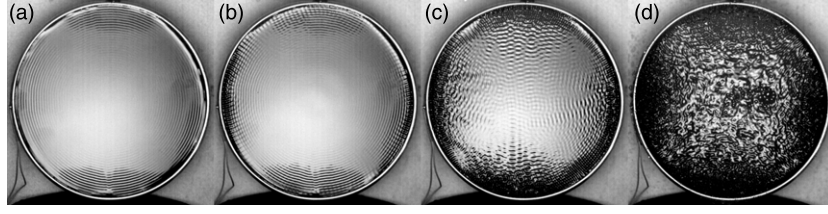


Figure 7. Evolution of the surface waves in Tibet 1 bowl filled with water and excited with a frequency $f = 188$ Hz corresponding to its fundamental mode (2,0). The amplitude of deformation is increasing from left to right: (a) $\Gamma = 1.8$, (b) $\Gamma = 2.8$, (c) $\Gamma = 6.2$, (d) $\Gamma = 16.2$.

3.3. Surface waves

Two different liquids were used in our experiment, pure water with density $\rho_w = 1000 \text{ kg m}^{-3}$, viscosity $\nu = 1 \text{ cSt}$ and surface tension $\sigma = 72 \text{ mN m}^{-1}$, and Dow Corning silicone oil with $\rho_o = 820 \text{ kg m}^{-3}$, $\nu = 1 \text{ cSt}$ and $\sigma = 17.4 \text{ mN m}^{-1}$. The fluid depth and resulting natural deformation frequencies of the bowl were varied. Specific deformation modes of the bowls were excited acoustically. We proceed by reporting the form of the flow induced, specifically, the evolution of the free surface with increasing rim forcing.

In figure 7 (and supplementary data movie 2 available at stacks.iop.org/Non/24/R51/mmedia), we present snapshots of the bowl Tibet 1 resonating in its fundamental deformation mode with different Γ when it is completely filled with water. The loudspeaker produces a sinusoidal sound at a frequency $f_0 = 188 \text{ Hz}$ that corresponds to the mode (2,0) with four associated nodes and antinodes. The vibration of the water surface is forced by the horizontal oscillation of the rim. When the amplitude of the rim oscillation is small, axisymmetric progressive capillary waves with frequency commensurate with the excitation frequency appear on the liquid surface. Although almost invisible to the naked eye, they can be readily detected by appropriate lighting of the liquid surface (figure 7(a)). When Γ is further increased, relatively large amplitude circumferential standing waves appear at the water's edge (figure 7(b) and supplementary data movie 3 available at stacks.iop.org/Non/24/R51/mmedia). These standing ripples, aligned perpendicular to the bowl's edge, are spaced by approximately a Faraday wavelength λ_F , as defined in (11). Moreover, their frequency is half that of the axial waves, indicating that these waves correspond to classic cross waves or, equivalently, edge-induced Faraday waves [14]. More complicated wave modes appear at higher excitation amplitude (figure 7(c)). At sufficiently high Γ , the Faraday waves break, and water droplets are ejected from the edge of the vessel (figure 7(d) and supplementary data movie 4 available at stacks.iop.org/Non/24/R51/mmedia), specifically from the antinodes of the oscillating wall. The ejected droplets may bounce, slide, and roll on the water surface before eventually coalescing.

One of our bowls (Tibet 2) resonates readily in both modes (2,0) and (3,0). When completely filled with water, the resonant frequencies of its (2,0) and (3,0) modes are $f = 144 \text{ Hz}$ and $f = 524 \text{ Hz}$, respectively. In figure 8, we observe the progression of the surface waves with increasing amplitude for each of these modes. Note that for the mode (3,0), since the frequency is higher, the wavelengths are shorter. Moreover, the sound amplitude needed to produce surface waves is necessarily higher for mode (3,0) than (2,0).

The transition from axisymmetric capillary waves to Faraday waves arises at a critical acceleration Γ_F readily measured by the accelerometer. This threshold was measured as a function of the forcing frequency, the latter having been tuned to excite the fundamental

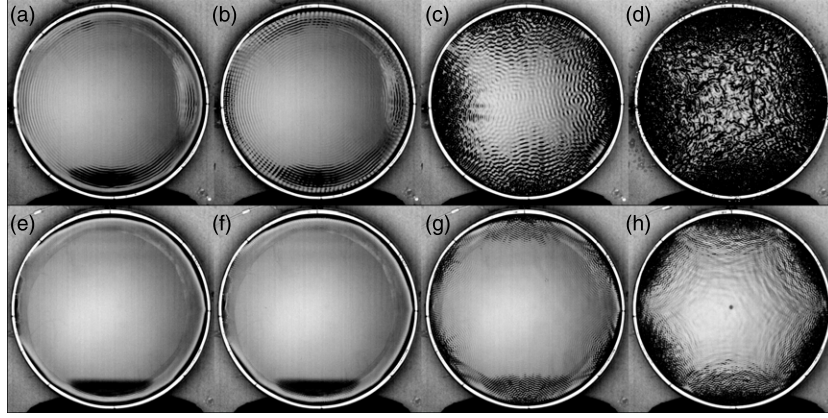


Figure 8. Evolution of the surface waves in Tibet 2 bowl filled with water. (a)–(d) Mode (2,0) is excited with a frequency $f = 144$ Hz. (e)–(h) Mode (3,0) is excited with $f = 524$ Hz. The amplitude of deformation is increasing from left to right. For the deformation mode $n = 2$, (a) $\Gamma = 1.0$, (b) $\Gamma = 1.7$, (c) $\Gamma = 5.0$, (d) $\Gamma = 12.7$. For the deformation mode $n = 3$, (e) $\Gamma = 5.7$, (f) $\Gamma = 7.7$, (g) $\Gamma = 15.1$, (h) $\Gamma = 33.8$.

deformation modes of the bowls with different liquid levels. We also measured this acceleration threshold for the deformation mode (3,0) of the bowl Tibet 2. Higher frequencies were explored with three different wine glasses filled to different levels using the strain gauge system. All the measurements with silicone oil of viscosity 1 cSt are presented in figure 9 (lower curve). Consistent with (13), the data suggest a dependence $\Gamma_F \propto f^{5/3}$. In figure 10(a), we report our measurements of Γ_F as a function of frequency for both silicone oil and distilled water. Each data set is fit by a 5/3 power law. Prefactors of 3.5×10^{-4} for water and 1.7×10^{-4} for 1 cSt silicone oil were inferred.

3.4. Surface fracture

When the Faraday waves become sufficiently large, they break, leading to droplet ejection. A second critical acceleration can thus be measured, Γ_d , above which droplets are ejected from the surface. The droplet ejection starts with very few droplets ejected, then the ejection rate increases with forcing amplitude. Our criterion for onset is that at least two droplets are ejected in a 15 s time interval. The dependence of Γ_d on f is presented in figure 9 (upper curve) for bowls and wine glasses filled with different levels of 1 cSt silicone oil. The drop ejection threshold scales as $\Gamma_d \propto f^{4/3}$, which is consistent with the scaling presented in (15).

In figure 10(b), our measurements of the dependence of Γ_d on f are reported for bowls filled with different levels of either 1 cSt silicone oil or water. The two Γ_d curves collapse when we use the scaling law (15) expected to apply for vertical forcing. Specifically, we find

$$\Gamma_d \sim 0.23(\sigma/\rho)^{1/3} f^{4/3}. \quad (16)$$

The droplet ejection acceleration threshold is thus in accord with measurements of Goodridge *et al* [23] and Puthenveetil and Hopfinger [22], even though our forcing is horizontal rather than vertical. Moreover, our prefactor is consistent with the results of both, who reported values between 0.2 and 0.3.

The diameter of the ejected droplets was measured for several forcing frequencies. The Tibetan bowls were fully filled with liquid, either 1 cSt silicone oil or pure water. Resonant deformation modes were then excited by the loudspeaker emitting sinusoidal signals at the

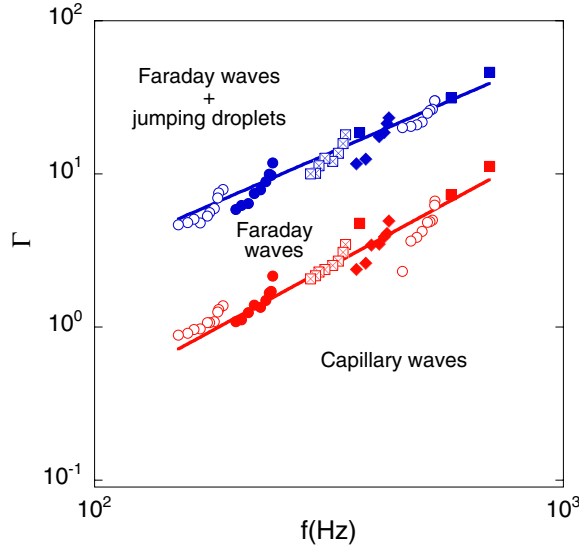


Figure 9. Phase diagram indicating the critical acceleration $\Gamma_F = \Delta\omega^2/g$ above which axial capillary waves give way to Faraday waves, and Γ_d above which the Faraday waves break. The \bullet , \circ , \boxtimes and \blacklozenge symbols correspond, respectively, to the measurements made with the bowls Tibet 1, 2, 3 4 and the \blacksquare to wine glasses filled with different levels of 1 cSt silicone oil. The first acceleration threshold (lower curve) scales as $\Gamma_F \propto f^{5/3}$ and the second (upper curve) as $\Gamma_d \propto f^{4/3}$.

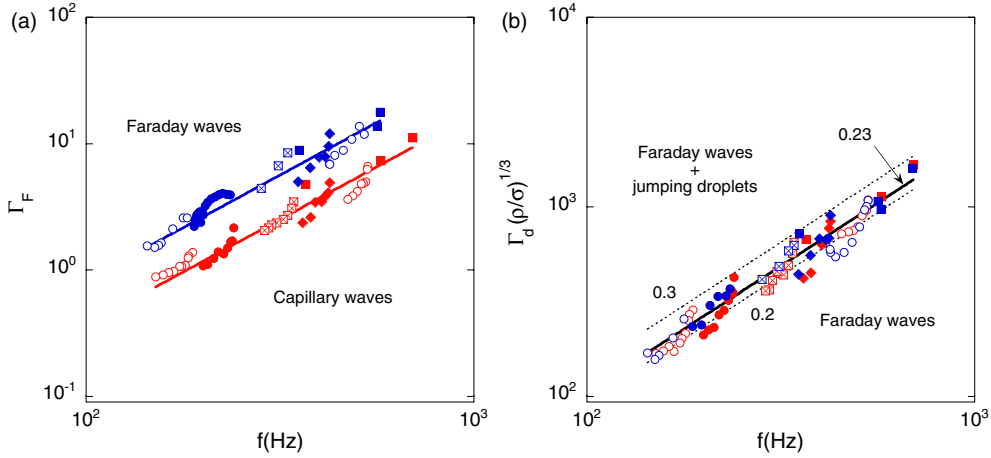


Figure 10. Dependence of acceleration thresholds on the frequency f for our vessels filled with different levels of pure water (blue symbols) and silicone oil of viscosity $\nu = 1$ cSt (red symbols). The \bullet , \circ , \boxtimes and \blacklozenge symbols correspond, respectively, to the measurements made with the bowls Tibet 1, 2, 3 4 and the \blacksquare to wine glasses. (a) Each data set of Faraday threshold measurements, Γ_F , is fit by a $5/3$ power law consistent with (13). (b) The droplet ejection threshold, Γ_d , is consistent with the scaling (15).

appropriate resonant frequency. The level of sound was adjusted so that the acceleration of the rim at the antinodes of the bowl were just above the threshold for droplet ejection, Γ_d . A high speed video camera (Phantom) was used to record the ejected droplets, from which drop size measurements were taken. We used a liquid-filled glass in order to extend the frequency range to 720 Hz. Soda cans have very thin walls, and very low resonant frequencies. We were thus

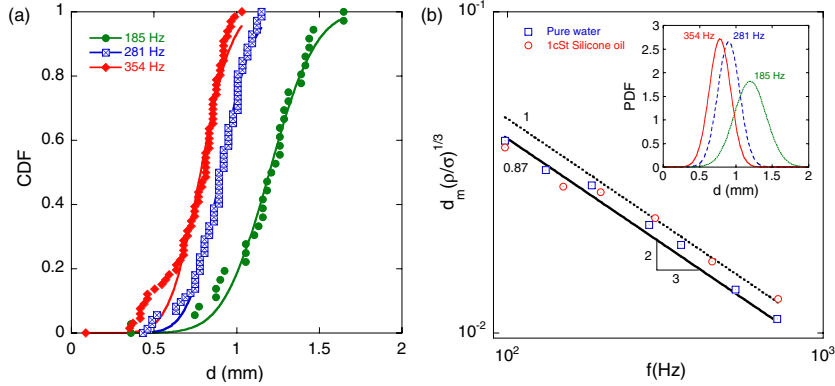


Figure 11. (a) Three cumulative distribution functions of ejected droplet sizes for the bowls Tibet 1, 3 and 4, fully filled with pure water and resonating in their fundamental deformation modes (2,0). The lines are the curves fit by an equation of a cumulative distribution function for the Gaussian distribution. (b) Mean size of the ejected droplets as a function of the frequency of the oscillating vessel, either a Tibetan bowl, wine glass or soda can. The two leftmost data points are from the measurements made with the soda cans, the two rightmost from the wine glass. Error bars are the size of our symbols. The black curve indicates a power law dependence with slope $-2/3$ and prefactor 0.87. The dotted line has the same slope, but a prefactor of 1. Inset: the corresponding Gaussian functions inferred from the cumulative distribution functions.

able to measure droplet sizes for the two liquids at a frequency of 98 Hz. Three cumulative distributions of ejected droplet sizes are presented in figure 11(a) for the bowls Tibet 1, 3 and 4 resonating in their fundamental deformation modes (2,0). Assuming that these distributions are Gaussian, appropriate fits to the cumulative distribution functions yield the parameters of the Gaussian distribution functions plotted in the inset of figure 11(b). The dependencies of the mean droplet size on the forcing frequency for the two liquids are presented in figure 11(b). Equation (14) adequately collapses our data, provided we choose a prefactor of 0.87. By way of comparison, Puthenveetil found 0.92 for their experiments with water, and 1.01 with Perfluoro-compound FC-72 liquid. Donnelly *et al* [45] found a prefactor of 0.98 from his measurements of aerosol water droplets.

3.5. Bouncing droplets

With a more viscous fluid (e.g. 10 cSt silicone oil), the waves are less pronounced, and the fluid is more strongly coupled to the vibrating sidewalls; specifically, more of the surface oscillates up and down near the wall's antinode. When a droplet of the same liquid is deposited on the surface, it may bounce, levitated by the underlying wave field. Such sustained levitation was not observed in the Tibetan singing bowl with liquid viscosities lower than 10 cSt.

In figure 12(a), we present a still image of a drop of diameter 0.5 mm bouncing on the liquid surface inside the bowl (Tibet 1) resonating at a frequency of $f_0 = 188$ Hz. The drop has been made by dipping then extracting a syringe needle, on the tip of which a capillary bridge forms and breaks, leaving a drop that bounces near the oscillating rim. A movie of the bouncing was recorded (see supplementary data movie 5 available at stacks.iop.org/Non/24/R51/mmedia), then vertical slices of each image through the droplet centreline juxtaposed. We can thus construct an image illustrating the dynamics of the droplet (figure 12(b)). In this case, the drop experiences two bounces of slightly different amplitude while the liquid surface (and the rim) oscillates twice. When a smaller droplet (of diameter 0.35 mm) is placed on the

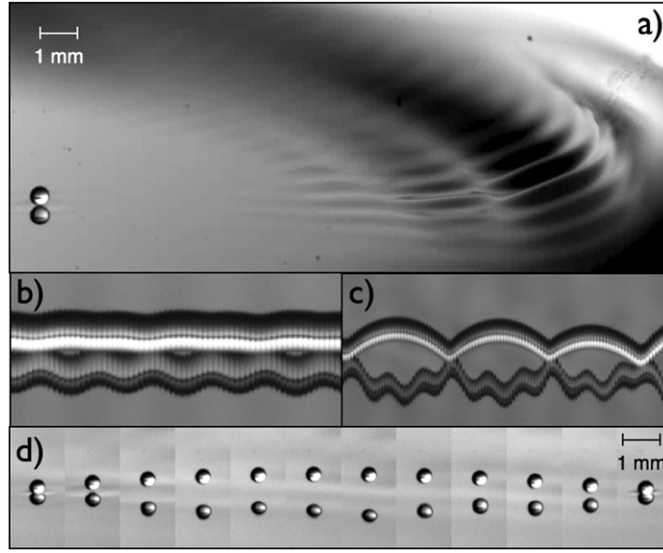


Figure 12. (a) Still image of a droplet of 0.5 mm diameter bouncing on a surface oscillating at 188 Hz, the frequency of the rim. Both droplet and bath are 10 cSt silicon oil. Spatio-temporal diagrams indicate the vertical trajectory of droplets of diameter (b) 0.5 mm and (c) 0.35 mm. Time elapses from left to right and the drop's reflection are apparent. (d) A single bounce of a droplet of diameter 0.35 mm is illustrated by an image sequence. Images are spaced by 1 ms.

oscillating surface, the bouncing motion can be more complex. In figure 12(c), we see that the droplet bounces only once during three oscillations of the surface. Figure 12(d) illustrates the corresponding trajectory. We note that the bouncing motion of sufficiently small drops can become chaotic.

We sought to sustain walking droplets in our system. Once the horizontal forcing amplitude Γ is just above the Faraday wave threshold Γ_F , circumferential Faraday waves are sustained at the edge of the vessel. Then, when Γ is increased, Faraday waves propagate progressively towards the centre of the vessel, their amplitude damped by viscosity. Beyond these waves, the liquid surface was quiescent unless perturbed by a bouncing droplet, in which case it could sustain a field of Faraday waves. This phenomenon was observed in the bowl Tibet 2 almost fully filled with 10 cSt silicone oil ($f_0 = 140$ Hz). Just beyond the Faraday waves, a bouncing droplet of diameter $500 \mu\text{m}$ was made such that its bouncing frequency corresponded to the Faraday wave frequency, that is, half the frequency of the vibrating rim. Such droplets were unable to excite sufficiently large Faraday waves to enable them to walk. We note that the usual range of walker diameters is between 650 and $850 \mu\text{m}$ [33, 34]: their mass is thus 4 times larger than that of our drops.

4. Conclusion

We have presented the results of an experimental investigation of the Tibetan singing bowl, its acoustics and hydrodynamics. Its acoustical properties are similar to those of a wine glass, but its relatively low vibration frequency makes it a more efficient generator of edge-induced Faraday waves and droplet generation via surface fracture.

Our observations of the bowl acoustics have been rationalized by adapting French's [1] theory of the singing wine glass. This model allowed us to characterize the bowl acoustics

and infer the Young modulus of the alloy constituting our antique bowls. The value we found, $Y = 77 \pm 6\%$ GPa, is in the range of glass, somewhat smaller than typical brass, copper or bronze alloys. This low value of Y and associated low resonant frequency is a critical component in the hydrodynamic behaviour of singing bowls: bowls with high fundamental frequencies are, like the wine glass, relatively inefficient generators of droplets.

Particular attention has been given to the Faraday waves produced when a critical acceleration of the horizontal rim oscillation is exceeded. These have been shown to be due to a destabilization of the axial capillary waves similar to those observed and studied theoretically [29, 24]. The acceleration threshold for droplet ejection has also been investigated and rationalized by simple scaling arguments. Droplet size was shown to be proportional to the Faraday wavelength, and our measurements were consistent with those on a vertically shaken liquid surface [22, 23, 45].

We have demonstrated that, following their creation via surface fracture, droplets may skip across or roll along the surface of fluid contained within a singing bowl. Moreover, careful choice of fluid properties and droplet position introduces the possibility of stable bouncing states reminiscent of those on a vertically driven free surface [30]. However, stable walking droplets and their concomitant quantum behaviour were not observed. Nevertheless, in developing hydrodynamic analogues of quantum systems, the edge-forcing examined here may be valuable in presenting a lateral gradient in proximity to Faraday threshold.

Acknowledgments

The authors thank Rosie Warburton for bringing this problem to our attention, and for supplying the bowls for our study. We are grateful to Jim Bales (of MIT's Edgerton Center), Barbara Hughey and Stéphane Dorbolo for assistance and fruitful discussions. Denis Terwagne thanks the University of Liège and the GRASP for financial support. This research was supported by the National Science Foundation through grant CBET-0966452.

References

- [1] French A 1983 In vino veritas—a study of wineglass acoustics *Am. J. Phys.* **51** 688
- [2] Chen K, Wang C, Lu C and Chen Y 2005 Variations on a theme by a singing wineglass *Europhys. Lett.* **70** 334
- [3] Chen Y-Y 2005 Why does water change the pitch of a singing wineglass the way it does? *Am. J. Phys.* **73** 1045
- [4] Jundt G, Radu A, Fort E, Duda J, Vach H and Fletcher N 2006 Vibrational modes of partly filled wine glasses *J. Acoust. Soc. Am.* **119** 3793
- [5] Courtois M, Guirao B and Fort E 2008 Tuning the pitch of a wine glass by playing with the liquid inside *Eur. J. Phys.* **29** 303
- [6] Arane T, Musalem A and Fridman M 2009 Coupling between two singing wineglasses *Am. J. Phys.* **77** 1066
- [7] Apfel R 1985 Whispering waves in a wineglass *Am. J. Phys.* **53** 1070
- [8] Rayleigh L 1945 *Theory of Sound* (Cambridge: Cambridge University Press)
- [9] Rossing T 1990 Wine glasses, bell modes and lord Rayleigh *Phys. Teach.* **28** 582
- [10] Rossing T 1993 Acoustics of the glass harmonica *J. Acoust. Soc. Am.* **95** 1106
- [11] Joubert S V, Fay T H and Voges E L 2007 A storm in a wineglass *Am. J. Phys.* **75** 647
- [12] Inacio O, Henrique L and Antunes J 2006 The dynamics of tibetan singing bowls *Acta Acust. United Acust.* **92** 637–53
- [13] Inacio O, Henrique L and Antunes J 2004 The physics of tibetan singing bowls (2004) *Rev. Acúst.* **35** 33–9
- [14] Faraday M 1831 On a peculiar class of acoustical figures; and on certain forms assumed by groups of particles upon vibrating elastic surfaces *Phil. Trans. R. Soc. Lond.* **121** 299–340
- [15] Rayleigh L 1883 On the crispations of fluid resting upon a vibrating support *Phil. Mag.* **16** 50
- [16] Benjamin T B and Ursell F 1954 The stability of the place free surface of a liquid in vertical periodic motion *Proc. R. Soc. Lond. A* **255** 505
- [17] Miles J and Henderson D 1990 Parametrically forced surface-waves *Annu. Rev. Fluid Mech.* **22** 143

- [18] Kumar K and Tuckerman L S 1994 Parametric instability of the interface between two fluids *J. Fluid Mech.* **279** 49
- [19] Edwards W and Fauve S 1994 Patterns and quasi-patterns in the faraday experiment *J. Fluid Mech.* **278** 123
- [20] Kudrolli A and Gollub J 1996 Patterns and spatiotemporal chaos in parametrically forced surface waves: A systematic survey at large aspect ratio *Physica D* **97** 133
- [21] Chen P and Vinals J 1997 Pattern selection in faraday waves *Phys. Rev. Lett.* **79** 2670
- [22] Puthenveetil B A and Hopfinger E J 2009 Evolution and breaking of parametrically forced capillary waves in a circular cylinder *J. Fluid Mech.* **633** 355
- [23] Goodridge C, Shi W T, Hentschel H and Lathrop D 1997 Viscous effects in droplet-ejecting capillary waves *Phys. Rev. E* **56** 472
- [24] Garrett C 1970 On cross-waves *J. Fluid Mech.* **41** 837
- [25] Barnard B J S and Pritchard W G 1972 Cross-waves: II. Experiments *J. Fluid Mech.* **55** 245
- [26] Mahony J J 1972 Cross-waves: I. Theory *J. Fluid Mech.* **55** 229
- [27] Miles J and Becker J 1988 Parametrically excited, standing cross-waves *J. Fluid Mech.* **186** 119
- [28] Becker J and Miles J 1991 Standing radial cross-waves *J. Fluid Mech.* **222** 471
- [29] Hsieh D 2000 Theory of water waves in an elastic vessel *Acta. Mech. Sin.* **16** 97
- [30] Couder Y, Fort E, Gautier C-H and Boudaoud A 2005 From bouncing to floating: noncoalescence of drops on a fluid bath *Phys. Rev. Lett.* **94** 177801
- [31] Gilet T, Terwagne D, Vandewalle N and Dorbolo S 2008 Dynamics of a bouncing droplet onto a vertically vibrated interface *Phys. Rev. Lett.* **100** 167802
- [32] Dorbolo S, Terwagne D, Vandewalle N and Gilet T 2008 Resonant and rolling droplet *New J. Phys.* **10** 113021
- [33] Protiere S, Couder Y, Fort E and Boudaoud A 2005 The self-organization of capillary wave sources *J. Phys. Condens. Matter* **17** S3529
- [34] Eddi A, Terwagne D, Fort E and Couder Y 2008 Wave propelled ratchets and drifting rafts *Eur. Phys. Lett.* **82** 44001
- [35] Gilet T and Bush J W M 2009 The fluid trampoline: droplets bouncing on a soap film *J. Fluid Mech.* **625** 167
- [36] Eddi A, Sultan E, Moukhtar J, Fort E, Rossi M and Couder Y 2011 Information stored in faraday waves: the origin of a path memory *J. Fluid Mech.* **674** 433–63
- [37] Couder Y and Fort E 2006 Single-particle diffraction and interference at a macroscopic scale *Phys. Rev. Lett.* **97** 154101
- [38] Eddi A, Fort E, Moisy F and Couder Y 2009 Unpredictable tunneling of a classical wave-particle association *Phys. Rev. Lett.* **102** 240401
- [39] Fort E, Eddi A, Boudaoud A, Moukhtar J and Couder Y 2010 Path-memory induced quantization of classical orbits *Proc. Natl Acad. Sci.* **107** 17515
- [40] Bush J W M 2010 Quantum mechanics writ large *Proc. Natl Acad. Sci.* **107** 17455
- [41] Perrin R, Charcley T, Banut H and Rossing T D 1985 Chladni's law and the modern English church bell *J. Sound Vib.* **102** 11
- [42] Kinsler L, Frey A, Coppers A and Sanders J 1982 Fundamentals of acoustics 3rd edn (New York: Wiley)
- [43] Akay A 2002 Acoustics of friction *J. Acoust. Soc. Am.* **111** 1525
- [44] Douady S 1990 Experimental study of the faraday instability *J. Fluid Mech.* **221** 383
- [45] Donnelly T, Hogan J, Mugler A, Schommer N, Schubmehl M, Bernoff A and Forrest B 2004 An experimental study of micron-scale droplet aerosols produced via ultrasonic atomization *Phys. Fluids* **16** 2843